

Cathodoluminescence of oval defects in GaAs/Al_xGa_{1-x}As epilayers using an optical fiber light collection system

Michael E. Hoenk and Kerry J. Vahala

Department of Applied Physics, 128-95, California Institute of Technology, Pasadena, California 91125

(Received 4 May 1988; accepted for publication 14 September 1988)

A cathodoluminescence system using a novel optical fiber light collection system is employed to study oval defects in GaAs/Al_xGa_{1-x}As epilayers grown by molecular beam epitaxy. Spatially and spectrally resolved data on the luminescence of oval defects are presented. Oval defects are found to contain an enhanced concentration of gallium, which is consistent with current theories regarding the origin of these defects.

Cathodoluminescence (CL) is a powerful tool for the study and characterization of small features in direct gap semiconductors with regard to their spectral emission. We have designed and built a CL system for a scanning electron microscope (SEM) using an optical fiber for collecting and guiding light out of the sample chamber. Our system is capable of both spatial and spectral resolution of the CL signal. In this letter we report the use of this system to study oval defects in GaAs/Al_xGa_{1-x}As epilayers grown by molecular beam epitaxy (MBE). We find that the defects studied exhibit a local shift of the Al_xGa_{1-x}As peak to longer wavelengths. Previous studies of the luminescence of oval defects either used samples without Al_xGa_{1-x}As epilayers or did not spectrally resolve the signal.¹⁻³

An electron beam scanning a sample will generate a variety of excitations. Among these are electron-hole pairs, some of which recombine by emitting a photon. The cathodoluminescence imaging technique uses these photons for image generation. A CL light collection system must be efficient and yet must not impair other detection apparatus, such as the secondary-electron detector. To achieve these goals, we have designed a system which utilizes an optical fiber for direct collection of light from the surface of the sample. The fiber is small enough so that access to the sample by other detection systems is not restricted. The optical fiber is positioned relative to the sample with externally controlled motorized translation stages. The fiber core is 200 μm in diameter, and its numerical aperture is 0.2. From this we find the optimum fiber to sample distance is 0.5 mm. Light from the fiber is focused onto the entrance slit of a monochromator and detected with a photomultiplier. After being amplified, the signal may be used to generate a CL image by feeding it directly into the auxiliary input of the SEM. Using this configuration, the monochromator acts as a bandpass filter for the light, and we obtain spectrally resolved cathodoluminescence (SRCL) images. Alternatively, we can use the electron beam as a movable probe for localized excitation of carriers. We then scan the monochromator and plot the local luminescence spectrum.

The most common macroscopic defects in the growth of III-V semiconductors by MBE are oval defects. On a (100) wafer, they are oriented with their long axis parallel to the [01 $\bar{1}$] direction. The shape of an oval defect is probably due to a tendency of facets to propagate away from raised disturbances in the [01 $\bar{1}$] direction and to propagate nearly vertically in the [011] direction.⁴

The first sample studied was a doped quantum well structure, MBE growth No. 562. The basic features of the structure are a 130 Å quantum well bounded by a 500 Å *p*-doped Al_{0.3}Ga_{0.7}As surface layer and a 0.64 μm *n*-doped Al_{0.3}Ga_{0.7}As layer. Beneath this structure is a five-period superlattice 0.12 μm wide and a 0.75 μm *n*-doped GaAs layer. The oval defects in this sample are distributed uniformly over the surface of the wafer, with a density of 4 × 10⁵ cm⁻². The defects are almost exclusively of the same type, having a spiked shape with a pit in the center. Most are about 3 μm long and half as wide, but there are some smaller defects with less well defined features. Optical photographs using Nomarski phase contrast show that the defects are surrounded by a sloping area terminated in a circle about 10 μm in diameter. For some of the defects in our sample, the pit is partially or completely overgrown with a faceted central feature, but none were observed to contain macroscopic particle inclusions.

The defects in this growth appear to have originated in the vicinity of the superlattice. Cross-sectional SEM micrographs of the sample show a pair of triangular bumps in the Al_xGa_{1-x}As layer beneath the defects, originating in the superlattice. In some cases there is a small bend in the superlattice underneath the defect. Micrographs taken by cross-sectional transmission electron microscopy (TEM) of two defects show a bending of the top layer of the superlattice, although the lower layers appear to be straight. Underneath the center of one of the defects observed by TEM, the micrographs show a light triangular region with its base in the superlattice and its apex 0.4 μm beneath the center of the defect.

SRCL imaging of the oval defects in MBE growth No. 562 reveals a dramatic spatial dependence of the spectral emission (Figs. 1 and 2). Since 20 keV electrons have a range of about 2 μm in GaAs, the luminescence reveals information about the spectral properties of material in an interaction volume which penetrates beneath the surface and spreads laterally around the point of entry into the sample.^{5,6}

Comparison of the SRCL micrographs at 7000 Å [Figs. 1(b) and 2(b)] with the secondary-electron images [Figs. 1(a) and 2(a)] shows that, at this wavelength, luminescence from the defects is enhanced within a halo surrounding the defect core. Spectra taken from this region show that the halo results from a local shift in the Al_xGa_{1-x}As emission peak relative to defect-free areas of the sample. The size of the halo region corresponds roughly to a sloping area

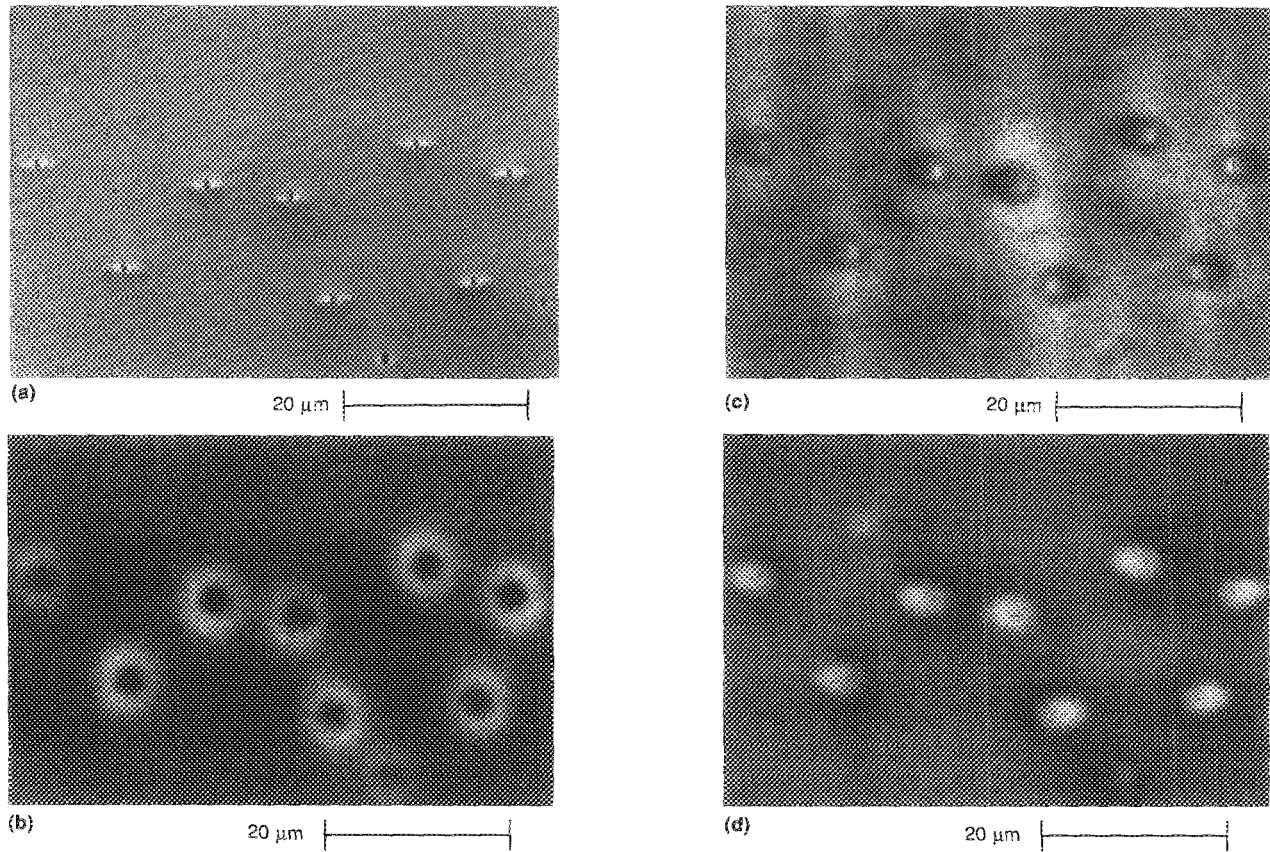


FIG. 1. Spectrally resolved cathodoluminescence (SRCL) images of oval defects in MBE growth No. 562: (a) SEM image; (b) SRCL image at 7000 Å; (c) SRCL image at 7600 Å; (d) SRCL image at 8500 Å.

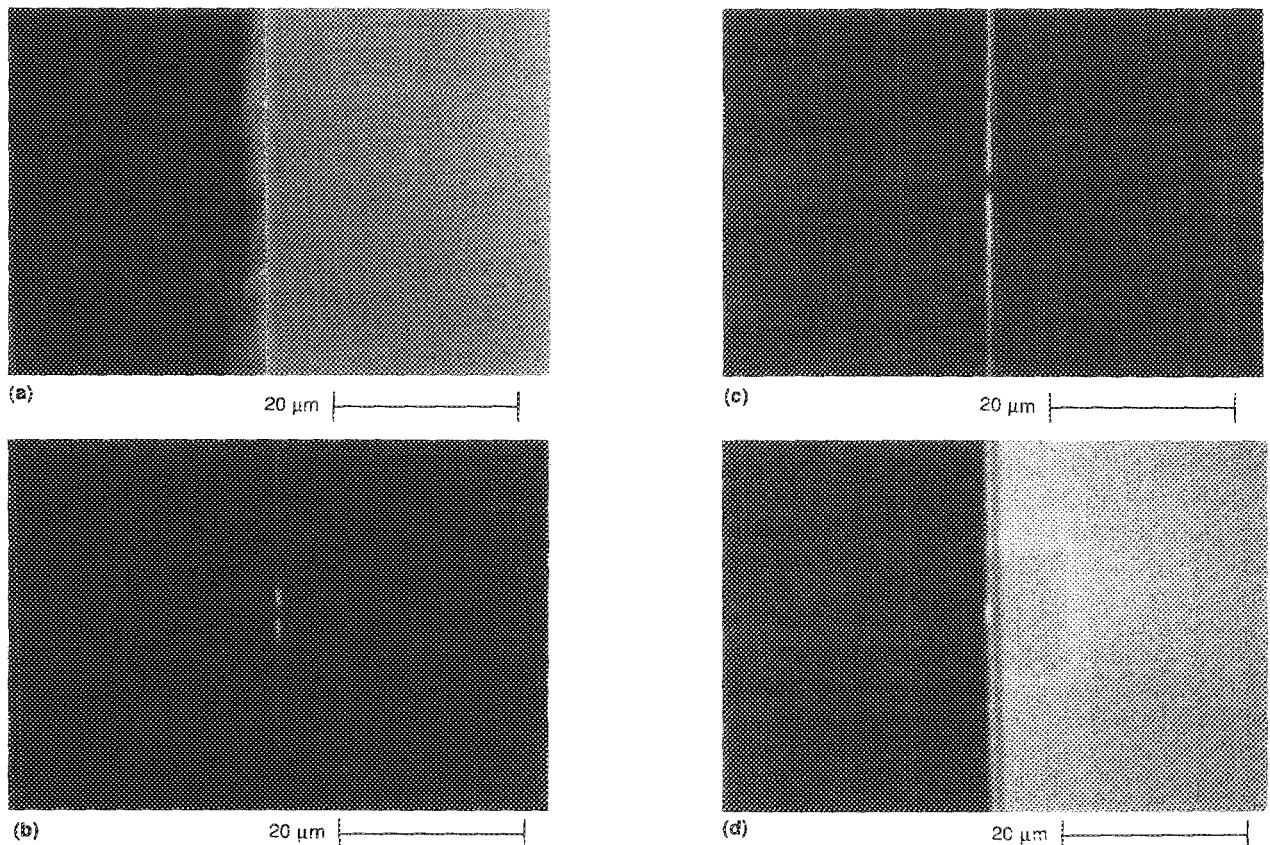


FIG. 2. Spectrally resolved cathodoluminescence (SRCL) images of oval defects in cross sections of MBE growth No. 562: (a) SEM image; (b) SRCL image at 7000 Å; (c) SRCL image at 7700 Å; (d) SRCL image at 8300 Å.

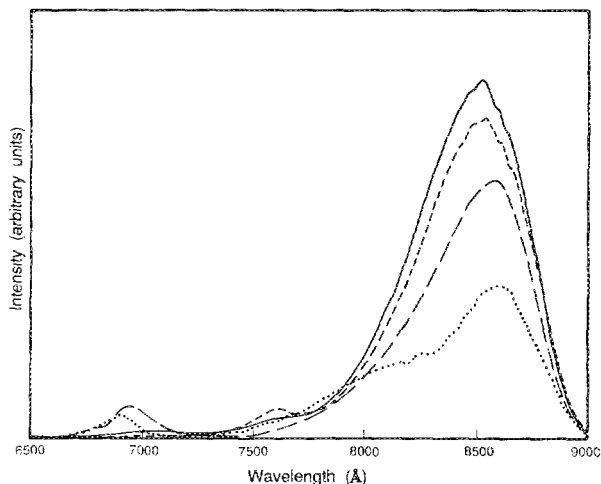


FIG. 3. Cathodoluminescence spectra from local excitation of carriers in oval defects of MBE growth No. 562: (a) solid line: defect core; (b) short dashes: lip of defect, $0.5 \mu\text{m}$ from core; (c) long dashes: halo, $2.3 \mu\text{m}$ from core; (d) dotted line: far from defect.

around similar defects observed by optical microscopy. Unfortunately, the slope is too gradual to appear in the micrographs taken with the scanning electron microscope.

The centers of the oval defects appear dark in the wavelength range from 6600 to 7100 Å. At about 7600 Å, the defect center luminesces strongly, whereas the halo becomes dark [Figs. 1(c) and 2(c)]. CL spectra show a localized peak at 7600 Å in the vicinity of the defect core (Fig. 3). This feature does not appear in defect-free regions of the sample.

Figures 1(d) and 2(d) show that the defects luminesce more brightly than the surrounding regions at the quantum well emission peak. Comparison of the quantum well emission peak in the CL spectra at various points around the defect shows that with increasing distance from the core, the intensity of the peak decreases and the peak shifts to longer wavelengths (Fig. 3). Defects in some areas of the sample did not exhibit enhanced luminescence intensity at the quantum well peak. These defects were also distinguished by a diamond-shaped area in their center which was dark at the quantum well peak.

The second sample studied, MBE growth No. 775, consisted of a $0.1 \mu\text{m}$ GaAs buffer layer, and a $2.3 \mu\text{m}$ n -doped $\text{Al}_{0.1}\text{Ga}_{0.9}\text{As}$ layer grown on a semi-insulating GaAs substrate. Five different types of defects were studied in this sample, one of which has the same external appearance as the defects in MBE growth No. 562. The details of the CL characteristics of these defects will be presented in a forthcoming publication. In all five types, the $\text{Al}_x\text{Ga}_{1-x}\text{As}$ peak was shifted from 8200 to 8600 Å either in the core or around the edges of large irregular growth features in the core. The appearance of the luminescence peak at 8600 Å was accompanied by a local reduction in the amplitude of the 8200 Å peak. Spectra taken at various points around these defects

show that the 8600 Å peak appears only in the vicinity of the defect. CL spectra from a cross section of the sample show that the 8600 Å peak comes from the epilayers, not the substrate.

Our observation of a local shift in the $\text{Al}_x\text{Ga}_{1-x}\text{As}$ peak to longer wavelengths could be explained by an enhanced concentration of gallium in the defect core. This is consistent with proposed mechanisms for the origin of defects involving localized accumulation of excess gallium during the growth. Such mechanisms include spitting of gallium from the effusion cell,⁷ nucleation of gallium droplets by a chemical reaction of Ga_2O formed in the Ga effusion cell,⁸⁻¹⁰ and gallium agglomeration around a particle on the wafer surface.¹¹⁻¹³

In conclusion, we have demonstrated a novel CL detection system using an optical fiber for light collection. We used spatially and spectrally resolved CL to probe the structure of oval defects in two GaAs/ $\text{Al}_x\text{Ga}_{1-x}\text{As}$ samples grown by MBE. Shifts in the $\text{Al}_x\text{Ga}_{1-x}\text{As}$ peak to longer wavelengths were found to occur in the vicinity of oval defects. In one of the samples, SRCL micrographs showed a bright halo surrounding the defects which corresponded to a gently sloping area around each of the defects. The spectral shift in this region was much smaller than the spectral shift observed in the center of the defects. These shifts in the $\text{Al}_x\text{Ga}_{1-x}\text{As}$ emission peak indicate an enhanced concentration of gallium in oval defects.

The authors would like to express their appreciation to Hadis Morkoç and Lars Eng for many helpful discussions. This work was supported by the Office of Naval Research and by Caltech's Program in Advanced Technologies, sponsored by Aerojet General, General Motors, and TRW.

- ¹M. Baffeur, A. Munoz-Yague, N. Lauret, and J. C. Brabant, *J. Cryst. Growth* **66**, 472 (1984).
- ²M. Cocito, P. Franzosi, G. Salviati, and F. Taiariol, *Scanning Electron Microscopy/1986/IV* (SEM Inc., AMF O'Hare, Chicago, IL, 1986), pp. 1299-1310.
- ³After the submission of this letter, it came to the author's attention that the results of another study on cathodoluminescence of oval defects were published recently [A. C. Papadopoulos, F. Alexandre, and J. F. Bresse, *Appl. Phys. Lett.* **52**, 224 (1988)].
- ⁴J. S. Smith, "III-V Molecular Beam Epitaxy Structures for Electronic and Opto-electronic Applications," Ph.D. thesis, Caltech, Dept. of Appl. Phys., 1986.
- ⁵R. U. Martinelli and C. C. Wang, *J. Appl. Phys.* **44**, 3350 (1973).
- ⁶C. D. W. Wilkinson and S. P. Beaumont, *Superlatt. Microstruct.* **2**, 587 (1986).
- ⁷C. E. C. Wood, L. Rathbun, H. Ohno, and D. DeSimone, *J. Cryst. Growth* **51**, 299 (1981).
- ⁸Young G. Chai and Robert Chow, *Appl. Phys. Lett.* **38**, 796 (1981).
- ⁹G. D. Pettit, J. M. Woodall, S. L. Wright, P. D. Kirchner, and J. L. Freeouf, *J. Vac. Sci. Technol. B* **2**, 241 (1984).
- ¹⁰K. Akimoto, M. Dohsen, M. Arai, and N. Watanabe, *J. Cryst. Growth* **73**, 117 (1985).
- ¹¹Shang-Lin Weng, C. Webb, Y. G. Chai, and S. G. Bandy, *Appl. Phys. Lett.* **47**, 391 (1985).
- ¹²S. Matteson and H. D. Shih, *Appl. Phys. Lett.* **48**, 47 (1986).
- ¹³Shang-Lin Weng, *Appl. Phys. Lett.* **49**, 345 (1986); *J. Vac. Sci. Technol. B* **5**, 725 (1987).